Non-steady-state kinetic studies of the real kinetic isotope effects and Arrhenius activation parameters for the proton transfer reactions of 9,10-dimethylanthracene radical cation with pyridine bases †

Yixing Zhao, Yun Lu and Vernon D. Parker *

Department of Chemistry and Biochemistry, Utah State University, Logan, UT 843222-0300, USA

Received (in Cambridge, UK) 12th March 2001, Accepted 29th May 2001
First published as an Advance Article on the web 6th July 2001

The kinetics of the reactions between 9,10-dimethylanthracene radical cation and 2,6-diethylpyridine (DEP) in dichloromethane–Bu_4NPF_6 (0.2 M) as well as that with 2,6-dimethylpyridine (LUT) in acetonitrile–Bu_4NPF_6 (0.1 M) were studied at temperatures ranging from 252 to 312 K. In the time period before steady-state was reached for both reaction systems at all temperatures, the apparent deuterium kinetic isotope effects (KIE_{app}) were observed to increase with extent of reaction. The KIE_{app}–extent of reaction profiles provide strong evidence for a two-step mechanism [eqns. (i),(ii)] consisting of reversible complex formation prior to rate determining proton transfer.

(i) $ArCH_3^{+\bullet} + B \rightleftharpoons ArCH_3^{+\bullet}/B$ $K_{eq} = k_f/k_b$

(ii) $ArCH_3^{+\bullet}/B \rightarrow ArCH_2^{\bullet} + BH^+$ k_p

(iii) $ArCH_2^{\bullet} + ArCH_3^{+\bullet} + B \rightarrow$ Products fast

Resolution of the kinetics into the relevant microscopic rate constants resulted in real deuterium kinetic isotope effects (KIE_{real}) which are much larger than KIE_{app} and were observed to increase markedly with decreasing temperature. Values of KIE_{real} ranged from 62 to 247. It is concluded that a significant degree of quantum mechanical tunneling is involved for both reaction systems. Activation parameters for apparent and microscopic rate constants are discussed with reference to the proton tunneling effect.

Introduction

Proton transfer reactions of organic radical cations have received a great deal of attention from both a kinetic[1–9] and a thermodynamic[10,11] viewpoint. The most important difference between this class of carbon acids and those encountered in earlier studies is that the radical cations are often very much stronger acids and are sometimes super-acids. When the acidic hydrogens reside on carbon the radical cations react at moderate rates even with relatively strong bases. The latter allows detailed kinetic studies to be carried out using transient techniques.

Radical cations are also subject to nucleophilic attack by both anionic and neutral nucleophiles.[12–15] It was recently pointed out that only nucleophilic attack at the 10-position is observed for the reaction of 9-methylanthracene radical cation with pyridine, but that when the base is 2,6-dimethylpyridine (LUT) initial nucleophilic attack at the 10-position is followed by elimination of lutidinium ion to give the 9-anthracenylmethyl radical.[1h] When 9,10-dimethylanthracene radical cation is the proton donor the rate of nucleophilic attack is diminished and only proton transfer takes place during the reaction with LUT.

Small and sometimes negative Arrhenius activation energies are frequently encountered in both proton transfer[1e–i] and nucleophile combination[14a,b,d,f,h,j] reactions of radical cations. This has implicated complex, rather than single-step, mechanisms for these reactions. Intermediates have not been observed in any case and their structures are unknown. We have assumed that the intermediates in both classes of reactions are likely to be π-complexes and that all of these reactions follow the same general mechanism [eqn. (1)], where B(N) acts either as a base (B) or as a nucleophile (N).

$$\text{Radical Cation} + B(N) \rightleftharpoons (\pi\text{-complex}) \rightarrow \text{Products} \quad (1)$$

The acidic protons of interest are often on the side-chain of the radical cations derived from methylarenes. Since bases are generally nucleophilic it seems reasonable that the initial interaction with a radical cation will involve the most electrophilic center on the latter, the positive charge. A direct interaction between the C–H dipole, remote from the positive charge, and the base would appear less likely.

A major problem in differentiating between the mechanisms is that under steady-state conditions the mechanisms are kinetically indistinguishable with rate laws differing only in the definition of the apparent rate constants. However, we have recently discovered that, depending upon the relative values of the microscopic rate constants, reactions following the mechanism shown as reactions (2)–(4) frequently reach steady-

$$ArCH_3^{+\bullet} + B \rightleftharpoons ArCH_3^{+\bullet}/B \quad K_{eq} = k_f/k_b \quad (2)$$

$$ArCH_3^{+\bullet}/B \rightarrow ArCH_2^{\bullet} + BH^+ \quad k_p \quad (3)$$

$$ArCH_2^{\bullet} + ArCH_3^{+\bullet} + B \rightarrow ArCH_2B^+ + ArCH_3 \quad \text{fast} \quad (4)$$

† This paper is dedicated to the memory of Professor Lennart Eberson whose many contributions had an enormous influence on the chemistry of radical cations and on the work of one of the authors (V. D. P.).

DOI: 10.1039/b102320a

state late in the first half-life.[1i] During the pre-steady-state period the various rate constants affect the overall reaction rate to different degrees than implied by rate law (5). This gives

$$-\mathrm{d}[\mathrm{ArCH_3}^{+\bullet}]/\mathrm{d}t = 2(k_\mathrm{f}\,k_\mathrm{p}/(k_\mathrm{p} + k_\mathrm{b}))[\mathrm{ArCH_3}^{+\bullet}][\mathrm{B}] \quad (5)$$

rise to apparent kinetic isotope effects ($\mathrm{KIE_{app}}$) which vary significantly with the extent of reaction. The observation of extent of reaction dependent $\mathrm{KIE_{app}}$ for these reactions establishes two mechanistic facts; first, that the reactions do not follow the simple mechanism, and second, that steady-state is not yet achieved in the time period where $\mathrm{KIE_{app}}$ varies.

The concurrent fitting of theoretical data obtained by digital simulation to experimental data for the reactions of both $\mathrm{ArCH_3}^{+\bullet}$ and $\mathrm{ArCD_3}^{+\bullet}$ results in a unique set of rate constants; k_f, k_b, k_p^H and k_p^D.[1i] The mechanism shown as reactions (2)–(4) was demonstrated and rate constants were assigned for the reactions of two different substituted methylanthracene radical cations with LUT and 2,6-diphenylpyridine in dichloromethane –$\mathrm{Bu_4NPF_6}$ (0.2 M) at 291 K. That study demonstrated that real kinetic isotope effects ($\mathrm{KIE_{real}}$), equal to $k_\mathrm{p}^\mathrm{H}/k_\mathrm{p}^\mathrm{D}$, for all four reactions are much larger than $\mathrm{KIE_{app}}$ and can only be accounted for by invoking a considerable degree of quantum mechanical tunneling. It should be pointed out that the extent of reaction dependent $\mathrm{KIE_{app}}$ would go undetected treating the data in the conventional way, in which concentration–time profiles are fitted to linear relationships for first- or second-order kinetics. The latter strategy also assumes steady state for complex mechanisms, which revokes the opportunity to resolve the kinetics and assign microscopic rate constants.

We have recently shown that the pre-steady-state time period can be accessed during the stopped-flow study of the kinetics of the reaction between 1-nitro-1-(4-nitrophenyl)ethane (NNPE) with hydroxide ion in aqueous acetonitrile.[16] The experimental kinetic data for this reaction were observed to deviate significantly from that expected for the simple mechanism. The kinetics were resolved by concurrent fitting of experimental extent of reaction–time profiles for $\mathrm{NNPE_H}$ and $\mathrm{NNPE_D}$ to appropriate theoretical data for the complex mechanism. Real deuterium kinetic isotope effects ranging from 17 to 26 were observed, along with Arrhenius activation parameters consistent with extensive proton tunneling ($E_\mathrm{a}^\mathrm{D} - E_\mathrm{a}^\mathrm{H} = 2.8$ kcal mol^{-1}; $A^\mathrm{D}/A^\mathrm{H} = 4.95$).

Since the rate constant for a proton transfer step passing through a classical transition state is expected to be much more temperature dependent than that for the fraction of the reaction taking place by tunneling through the barrier, kinetic studies over a range of temperatures have been recommended in order to provide evidence for the latter.[17] In this paper we present kinetic results for the reactions of 9,10-dimethylanthracene radical cations ($\mathrm{DMA}^{+\bullet}$ and $\mathrm{DMA\text{-}d_6}^{+\bullet}$) with LUT and 2,6-diethylpyridine (DEP) as a function of temperature in dichloromethane–$\mathrm{Bu_4NPF_6}$ (0.2 M) and acetonitrile–$\mathrm{Bu_4NPF_6}$ (0.1 M). We have successfully resolved the kinetics and have assigned microscopic rate constants for all of the reactions over the entire temperature range studied and have evaluated $\mathrm{KIE_{real}}$ in all cases.

Results

The proton transfer reactions of $\mathrm{DMA}^{+\bullet}$ and $\mathrm{DMA\text{-}d_6}^{+\bullet}$ with DEP in dichloromethane–$\mathrm{Bu_4NPF_6}$ (0.2 M) and with LUT in accetonitrile–$\mathrm{Bu_4NPF_6}$ (0.1 M) were studied in the temperature range 252 to 312 K. The reaction kinetics were studied using derivative cyclic voltammetry (DCV)[18] and the rate constants were evaluated by fitting experimental DCV data to the theoretical data obtained by digital simulation[19] using the procedure recently described.[1i] Experimental DCV response curves were closely matched with theoretical data for the two-step proton transfer mechanism [eqns. (2)–(4)]. The proposed scheme is the simplest complex mechanism consistent with the experimental data. We cannot rule out the possibility of a more complex mechanism involving additional steps.

Assignment of rate constants

The magnitude of the ratio of the derivative peak heights ($R'_I = I'_\mathrm{b}/I'_\mathrm{f}$) is a measure of the rate of reaction of the electrode-generated intermediate, ranging from 1.0 for no reaction to 0 for complete reaction during the time of the experiment. The experimental variable is v, the voltage sweep rate. The experimental $R'_I/(1/v)$ response curves may be compared with theoretical data obtained by digital simulation in order to evaluate rate constants of the homogeneous chemical reactions coupled to the charge transfer reaction of the substrate.

The concurrent fitting of data for both $\mathrm{ArCH_3}^{+\bullet}$ and $\mathrm{ArCD_3}^{+\bullet}$ results in a unique set of rate constants which give the best correspondence between the experimental response and the theoretical data.[1i] In order to arrive at this unique set of rate constants, the parameters must be varied over a wide range in a systematic manner. Arriving at the unique set of rate constants requires a large number of simulations.

Our data fitting procedure involves calculating $(v_\mathrm{exp}^\mathrm{H} - v_\mathrm{sim}^\mathrm{H})^2/v_\mathrm{sim}^\mathrm{H}$, $(v_\mathrm{exp}^\mathrm{D} - v_\mathrm{sim}^\mathrm{D})^2/v_\mathrm{sim}^\mathrm{D}$, and $(\mathrm{KIE_{exp}} - \mathrm{KIE_{sim}})^2/\mathrm{KIE_{sim}}$, where v^H and v^D are the voltage sweep rates necessary for a particular R'_I and the subscripts refer to experimental (exp) and simulation (sim) data, at each R'_I from 0.85 down to 0.50 and summing each of these over the entire range (Σ_H, Σ_D, and Σ_KIE). Since the dependence of $\mathrm{KIE_{app}}$ on R'_I is the most important parameter in arriving at a unique fit, Σ_KIE is used directly in the data fit while Σ_H and Σ_D are monitored to assure that good fits to the two response curves are obtained.

The fact that the range of k_f over which R'_I-dependent $\mathrm{KIE_{app}}$ are observed is limited, *i.e.* from $k_\mathrm{app}^\mathrm{H}$ to $11(k_\mathrm{app}^\mathrm{H})$, suggests the following strategy. We typically select about 10 k_f over the applicable range starting at $k_\mathrm{app}^\mathrm{H}$ and determine the values of the other rate constants, k_p^H, k_b and k_p^D, which give the best fit for that particular k_f value. This is done by varying k_p^H and adjusting the other two rate constants (k_b and k_p^D) to conform to eqns. (6)–(8), where the subscript s.s. refers to

$$(k_\mathrm{app}^\mathrm{H})_\mathrm{s.s.}/2k_\mathrm{f} = (k_\mathrm{p}^\mathrm{H}/k_\mathrm{b})/(1 + k_\mathrm{p}^\mathrm{H}/k_\mathrm{b}) = C_\mathrm{H} \quad (6)$$

$$(k_\mathrm{app}^\mathrm{D})_\mathrm{s.s.}/2k_\mathrm{f} = (k_\mathrm{p}^\mathrm{D}/k_\mathrm{b})/(1 + k_\mathrm{p}^\mathrm{D}/k_\mathrm{b}) = C_\mathrm{D} \quad (7)$$

$$\mathrm{KIE_{real}} = [C_\mathrm{H}/(1 - C_\mathrm{H})]/[C_\mathrm{D}/(1 - C_\mathrm{D})] \quad (8)$$

steady-state. For each k_f a series of Σ_KIE as a function of k_p^H is obtained. Plots of Σ_KIE *vs.* k_p^H are parabola-like curves with minima that reflect the best fit of experimental to theoretical data for the k_f value. Fitting of experimental to theoretical data is best accomplished by using an iterative approach. The approximate rate constants obtained using moderate changes in the variables provide the starting point for more accurate fitting. The overall result is a series of the fitting parameter at the minimum ($(\Sigma_\mathrm{KIE})_\mathrm{min}$) as a function of k_f. A plot of $(\Sigma_\mathrm{KIE})_\mathrm{min}$ *vs.* k_f is, again, parabola-like, with a minimum which reflects the best value of k_f. The fitting procedure is illustrated graphically in Fig. 3 of reference 1*i*. The factor of 2 which appears on the left hand side of eqns. (6) and (7) is a consequence of the stoichiometry of reactions (2)–(4).

Temperature effects on experimental DCV data for the radical cation proton transfer reactions

The experimental DCV data for the reactions of $\mathrm{DMA}^{+\bullet}$ and $\mathrm{DMA\text{-}d_6}^{+\bullet}$ as a function of temperature are illustrated in Figs. 1 and 2 for both solvent–base systems. The solid symbols are for the $\mathrm{DMA}^{+\bullet}$ data and the open symbols are for the $\mathrm{DMA\text{-}d_6}^{+\bullet}$ data in both figures. The solid lines represent the

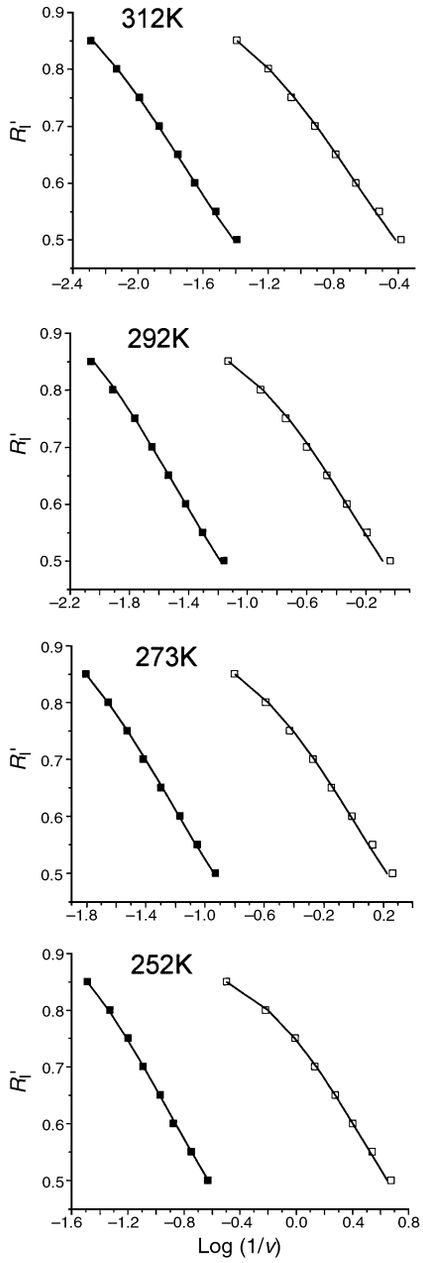

Fig. 1 DCV kinetic data for the reactions of $DMA^{+\bullet}$ (solid squares) and DMA-$d_6^{+\bullet}$ (open squares) with LUT in acetonitrile–Bu_4NPF_6 (0.1 M) as a function of temperature. The solid lines represent theoretical data for the complex proton transfer mechanism.

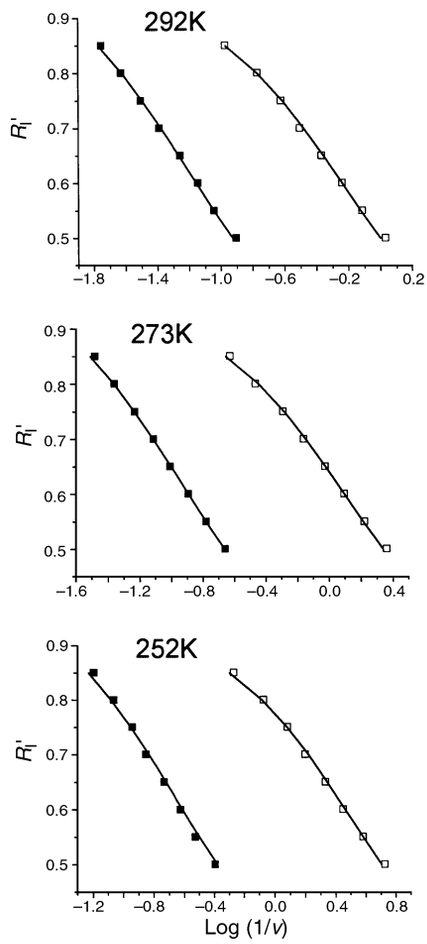

Fig. 2 DCV kinetic data for the reactions of $DMA^{+\bullet}$ (solid squares) and DMA-$d_6^{+\bullet}$ (open squares) with DEP in dichoromethane–Bu_4NPF_6 (0.2 M) as a function of temperature. The solid lines represent theoretical data for the complex proton transfer mechanism.

best-fit theoretical data obtained as described in the previous section. The most significant feature of these data is the fact that in all cases excellent correspondences between experimental and theoretical data for the mechanism shown by reactions (2)–(4) are observed.

Arrhenius plots of ln k *vs.* $1/T$, where k are k_{app}^{H}, k_{app}^{D}, k_p^{H}, and k_p^{D}, are illustrated for both solvent systems in Figs. 3 and 4. Again, the solid symbols refer to data for $DMA^{+\bullet}$ and the open symbols are for DMA-$d_6^{+\bullet}$ data. In all cases excellent linear relationships are observed over the limited temperature intervals.

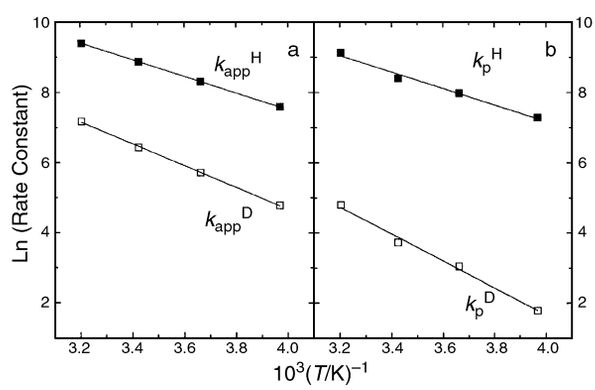

Fig. 3 Arrhenius plots for the reactions of $DMA^{+\bullet}$ (solid squares) and DMA-$d_6^{+\bullet}$ (open squares) with LUT in acetonitrile–Bu_4NPF_6 (0.1 M) derived from apparent rate constants (a) and microscopic rate constants (b).

The effect of extent of reaction on KIE_{app} for the proton transfer reactions of the radical cations

The experimental evidence which differentiates the mechanism shown as reactions (2)–(4) from a simple second-order proton transfer mechanism consists of the observation of a KIE_{app} dependent on the extent of reaction in the time period before steady-state is achieved. For the reactions studied here, this evidence is illustrated by the data in Tables 1 and 2 for the reactions of the radical cations with LUT in acetonitrile–Bu_4NPF_6 (0.1 M) and with DEP in dichloromethane–Bu_4NPF_6 (0.2 M), respectively. For these reactions, at all temperatures studied, KIE_{app} increases significantly with extent of reaction in the R_I' range from 0.85 down to 0.50. In Tables 1 and 2 both experimental (exp) and simulated (sim) KIE_{app} are listed. This again shows the excellent fit between experimental and theoretical data for the reactions over the entire range of temperature in the two solvent systems.

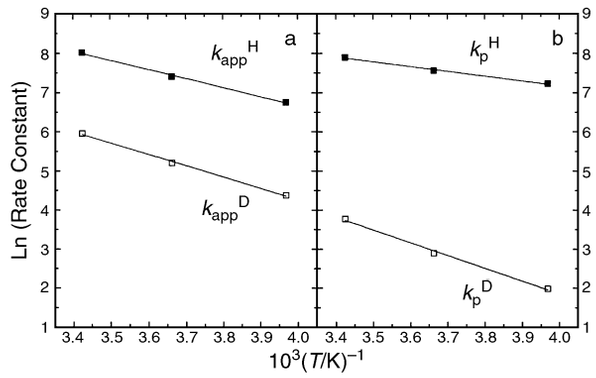

Fig. 4 Arrhenius plots for the reactions of $DMA^{+\bullet}$ (solid squares) and DMA-$d_6^{+\bullet}$ (open squares) with DEP in acetonitrile–Bu_4NPF_6 (0.1 M) derived from apparent rate constants (a) and microscopic rate constants (b).

The effect of temperature on apparent and real deuterium kinetic isotope effects

As expected, both KIE_{app} and KIE_{real} were observed to depend markedly on temperature. Rate constants for both reaction systems are summarized in Tables 3 and 4. The effect of temperature on KIE_{app} for the reactions of $DMA^{+\bullet}$ with LUT in acetonitrile–Bu_4NPF_6 (0.1 M) is similar to that observed above. However, KIE_{real} values in this case were larger and were found to vary from 76 to 247 in the temperature range from 312 to 252 K. For the reactions of the radical cations with DEP in dichloromethane–Bu_4NPF_6 (0.2 M) both the magnitude and the range of KIE_{app} increased with decreasing temperature. For this system, KIE_{real} varied from 62 to 189 as the temperature was decreased from 291 to 252 K.

Activation parameters for the reactions of DMA radical cations with pyridine bases

Arrhenius activation parameters for the reactions of $DMA^{+\bullet}$ and DMA-$d_6^{+\bullet}$ with LUT in acetonitrile–Bu_4NPF_6 (0.1 M) and DEP in dichloromethane–Bu_4NPF_6 (0.2 M) are gathered in Tables 5 and 6, respectively. The activation parameters apply to four distinct rate constants including k_{app}^{H}, k_{app}^{D}, k_p^{H} and k_p^{D} in the two solvent–base systems. Although there are differences, the activation parameters for the two reaction systems appear to be remarkably similar. The greatest differences are in the values of the Arrhenius *A* factors, which are consistently greater when the base is LUT (Table 5) as compared to that when DEP (Table 6) is the base. Binding energies in the intermediate complexes can be estimated from the temperature effect on the equilibrium constants (equal to k_f/k_b) for the formation of the complexes (Tables 3 and 4). The binding energies of the corresponding radical cation–base complexes were estimated from van't Hoff plots to be equal to −1.2 and −0.6 kcal mol^{-1} for LUT in acetonitrile–Bu_4NPF_6 (0.1 M) and DEP in dichloromethane–Bu_4NPF_6 (0.2 M), respectively.

Uncertainty in rate constants and kinetic isotope effects derived from the fitting procedure

The average deviations between experimental data and theoretical fitting lines, for example those illustrated in Figs. 1 and 2, are about 2%, which is within experimental error for

Table 1 Apparent (KIE_{app}, Exp = experimental, Sim = simulated) and real (KIE_{real}) deuterium kinetic isotope effects for the reactions of $DMA^{+\bullet}$ with LUT in acetonitrile–Bu_4NPF_6 (0.1 M) at different temperatures

	T/K							
	312		292		273		252	
R_I'	Exp	Sim	Exp	Sim	Exp	Sim	Exp	Sim
0.85	7.90	7.62	8.54	8.21	10.1	10.1	9.81	9.78
0.80	8.55	8.54	10.0	9.94	11.5	12.0	13.0	13.8
0.75	8.61	9.04	10.5	10.9	12.4	13.1	15.5	15.8
0.70	9.09	9.35	11.1	11.6	13.9	13.7	16.8	17.0
0.65	9.28	9.57	11.8	11.9	14.1	14.1	17.6	17.8
0.60	9.73	9.71	12.3	12.3	14.4	14.4	18.8	18.3
0.55	10.1	9.81	13.0	12.5	15.1	14.6	19.5	18.7
0.50	10.2	9.90	13.4	12.6	15.6	14.7	20.3	18.9
KIE_{real}	75.6		107		139		247	

Table 2 Apparent (KIE_{app}, Exp = experimental, Sim = simulated) and real (KIE_{real}) deuterium kinetic isotope effects for the reactions of $DMA^{+\bullet}$ with DEP in CH_2Cl_2–Bu_4NPF_6 (0.2 M) at different temperatures

	T/K					
	292		273		252	
R_I'	Exp	Sim	Exp	Sim	Exp	Sim
0.85	6.05	6.30	7.14	7.14	8.44	8.49
0.80	7.23	7.11	7.84	8.22	9.79	9.93
0.75	7.64	7.61	8.73	8.87	10.6	10.8
0.70	7.67	7.91	8.97	9.27	11.3	11.3
0.65	7.77	8.10	9.61	9.54	11.6	11.6
0.60	8.06	8.26	9.75	9.74	11.8	11.8
0.55	8.51	8.35	10.0	9.86	12.7	12.0
0.50	8.65	8.42	10.5	9.96	13.2	12.2
KIE_{real}	61.9		106		189	

Table 3 Rate constants for the reactions of $DMA^{+\bullet}$ with LUT in acetonitrile–Bu_4NPF_6 (0.1 M) at different temperatures[a,b]

T/K	k_{app}^{H}	k_{app}^{D}	k_p^{H}	k_p^{D}	k_f	k_b	k_{et}	KIE_{app}	KIE_{real}
312	12090	1307	9190	122.0	13960	1143	67200	7.90–10.2	75.6
292	7160	628	4430	41.4	7940	482	51500	8.54–13.4	107
273	4080	306	2930	21.1	4480	287	28700	10.1–15.8	139
252	1984	120	1470	5.95	2120	99.3	13520	9.81–20.3	247

[a] [DMA] = 1.0 mM and [LUT] = 10.0 mM. [b] Units for k_{app}^{H}, k_{app}^{D}, k_f and k_{et} are M^{-1} s^{-1}; units for k_p^{H}, k_p^{D} and k_b are s^{-1}.

Table 4 Rate constants for the reactions of $DMA^{+\bullet}$ with DEP in CH_2Cl_2–Bu_4NPF_6 (0.2 M) at different temperatures[a,b]

*T*K	k_{app}^{H}	k_{app}^{D}	k_p^{H}	k_p^{D}	k_f	k_b	k_{et}	KIE_{app}	KIE_{real}
292	3030	386.5	2690	43.5	3420	341	57100	6.05–8.65	61.9
273	1650	182.2	1912	18.04	1788	159.0	42200	7.14–10.5	106
252	860	79.6	1380	7.30	908	76.1	25300	8.44–13.2	189

[a] [DMA] = 0.5 mM and [DEP] = 12.5 mM. [b] Units for k_{app}^{H}, k_{app}^{D}, k_f and k_{et} are M^{-1} s^{-1}; units for k_p^{H}, k_p^{D} and k_b are s^{-1}.

Table 5 Arrhenius parameters for apparent and real proton and deuteron transfer reactions of $DMA^{+\bullet}$ with LUT in acetonitrile–Bu_4NPF_6 (0.1 M)

	Apparent[a]		Real[b]	
	H	D	H	D
E_a/kcal mol^{-1}	4.71	6.19	4.62	7.66
$E_a^D - E_a^H$/kcal mol^{-1}	1.48		3.04	
10^6A	23.8	27.7	14.0	25.6
A^D/A^H	1.04		1.83	

[a] From $k_{app}{}^H$ and $k_{app}{}^D$. [b] From $k_p{}^H$ and $k_p{}^D$.

Table 6 Arrhenius parameters for apparent and real proton and deuteron transfer reactions of $DMA^{+\bullet}$ with DEP in CH_2Cl_2–Bu_4NPF_6 (0.2 M)

	Apparent[a]		Real[b]	
	H	D	H	D
E_a/kcal mol^{-1}	4.60	5.76	2.43	6.50
$E_a^D - E_a^H$/kcal mol^{-1}	1.16		4.07	
10^6A	8.13	7.72	0.173	3.05
A^D/A^H	0.950		17.6	

[a] From $k_{app}{}^H$ and $k_{app}{}^D$. [b] From $k_p{}^H$ and $k_p{}^D$.

Table 7 The effect of fitting errors in rate constants on the quality of experimental to theoretical R_I' – sweep data fits[a]

Rate constant	Δ_{total}	Δ_H	Δ_D	Δ_{KIE}
Best fit	6.58	1.24	2.17	3.17
$(k_{app}{}^H/M^{-1}\ s^{-1}) + 1\%$	12.13	1.53	5.18	5.42
$(k_{app}{}^H/M^{-1}\ s^{-1}) - 1\%$	13.32	1.50	5.68	6.14
$(k_{app}{}^D/M^{-1}\ s^{-1}) + 1\%$	7.04	1.24	2.60	3.19
$(k_{app}{}^D/M^{-1}\ s^{-1}) - 1\%$	7.13	1.24	2.55	3.33
$(k_f/M^{-1}\ s^{-1}) + 1\%$	12.69	1.24	5.39	6.07
$(k_f/M^{-1}\ s^{-1}) - 1\%$	12.29	1.24	5.14	5.91
$(k_p{}^H/s^{-1}) + 10\%$	10.88	1.22	4.42	5.24
$(k_p{}^D/s^{-1}) - 10\%$	9.08	1.27	3.63	4.18
$(k_{et}/M^{-1}\ s^{-1}) + 10\%$	7.21	1.25	2.55	3.42
$(k_{et}/M^{-1}\ s^{-1}) - 10\%$	6.91	1.23	2.50	3.18

[a] Data from the reaction of $DMA^{+\bullet}$ with LUT in acetonitrile–Bu_4NPF_6 (0.2 M).

the measurement of R'_I. The deviations of experimental and theoretical KIE_{app} (Tables 1 and 2), which are the ratios of the H and D points in Figs. 1 and 2, are slightly greater, at about 3%, but also within experimental error by virtue of the data from which they are derived.

The effect of changes in rate constants on the percent deviations between experimental and theoretical data is illustrated in Table 7. The first row in Table 7 summarizes the various percent deviations, Δ_{total}, Δ_H, Δ_D and Δ_{KIE} [eqn. (9)] for the

$$\Delta_{total} = \Delta_H + \Delta_D + \Delta_{KIE} \quad (9)$$

best fit between experimental points measured at 291 K for the reaction between $DMA^{+\bullet}$ with LUT in acetonitrile–Bu_4NPF_6 (0.1 M) and theoretical data for the complex mechanism. The terms on the right-hand side of eqn. (9) refer to the percent deviation between experimental and theoretical data for the R'_I–v profiles for proton transfer (Δ_H), deuteron transfer (Δ_D) and that for KIE_{app}(Δ_{KIE}). The remaining lines in the table show the effect of varying a single rate constant in the simulations while holding all others at the value of the best fit. Plots of any one of the percent deviations *vs.* one of the rate constants are parabola-like, with the best fit value at the minimum.[1i] How shallow or how deep the parabola are depends upon which rate constant is plotted. From the data in Table 7 it is obvious that

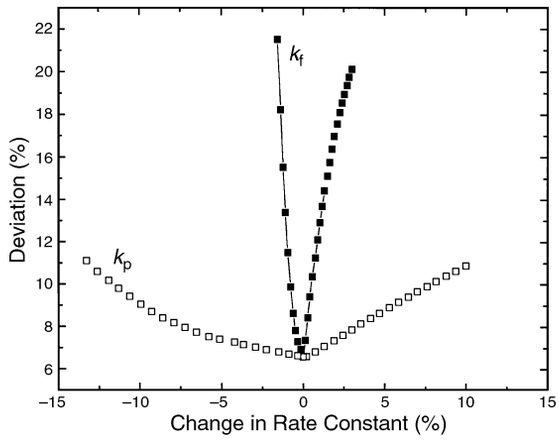

Fig. 5 Plots showing percent deviation of theoretical to experimental data caused by changes in rate constants from the best-fit values; k_f (solid squares) and k_p (open squares).

Δ_{total} is much more sensitive to changes in k_f, $k_{app}{}^H$ and $k_{app}{}^D$ than to changes in k_p.

The difference in sensitivity toward changes in k_f and k_p is further illustrated by the Δ_{total} *vs.* rate constant profiles in Fig. 5. The data near the minima of the curves are parabola-like and may be fit with second-order polynomial equations. The k_f plot is very narrow and steep and any departure from the best-fit value of k_f results in significant change in the % deviation. The k_p plot is much broader and more shallow; changes in k_p from the best fit value result in smaller changes in the % deviation. When the x-axis is expressed in rate constant values this suggests that the fitting error would be smaller for k_f than for k_p. However, the minimum can be located for both of the plots with very small degrees of uncertainty.

We use two different methods to locate the best fit depending upon the stage of refinement of the fit. The first method, which is used at a lower degree of fit refinement, is to select the lowest value of the fitting parameter for a series of simulations. The second, more accurate, method is to treat the data close to the minima as second-order polynomials and to calculate the rate constants at the minima from the equations of the lines. The latter method is used in the final stages of the fitting procedure. For the data shown in Fig. 5, the difference in best fit rate constants using the two different methods of finding the minima is negligible. We find that Δ_{total} is generally very sensitive to changes in k_f from the best fit value. This is of importance, since KIE_{real} only depends on k_f and the experimental apparent rate constants [eqn. (8)].

Discussion

General reactions (2) and (3) are illustrated in Scheme 1 using the reaction between of $DMA^{+\bullet}$ and LUT as an example. The proton transfer step (3) is followed by rapid product forming reactions (4). An important feature of the reaction is that proton transfer is irreversible due to the large equilibrium constant and the rapid product-forming reactions of the generated free radical.[1h] We have previously shown[1i] that kinetic data for this, and several related reactions, are inconsistent with a simple second-order mechanism for the proton transfer reaction. The mechanism illustrated in Scheme 1 was assigned on the basis of fitting experimental to theoretical data in the pre-steady-state period where KIE_{app} were observed to vary significantly with the extent of reaction.

The application of non-steady-state kinetics provides the means to resolve the kinetics of proton transfer reactions passing through the mechanism shown as reactions (2)–(4).[1i] In the time window before steady-state is achieved, rate equation (5) is not yet applicable and the relative effect of the

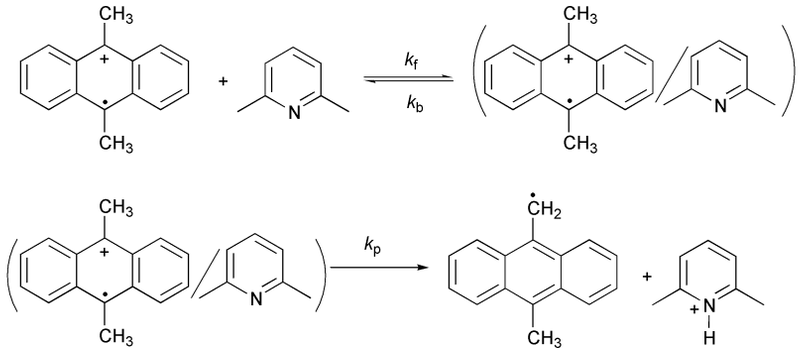

Scheme 1

microscopic rate constants differ from that at steady-state. An experimental observation characteristic of this situation is KIE_{app} that deviate significantly from the steady-state value at small extent of reaction, converging to it as the reaction progresses. The data in Tables 1 and 2 demonstrate the variations in KIE_{app} for the radical cation proton transfer reactions during the *pre-steady-state* period.

Besides demonstrating that the complex proton transfer mechanism [reactions (2)–(4)] rather than a simple second-order mechanism is applicable, the extent of reaction dependence of KIE_{app} also serves as the experimental tool to resolve the kinetics into the microscopic rate constants for the various steps.[1i] The R'_I *vs.* log (1/*v*) profiles shown in Figs. 1 and 2 demonstrate the goodness of fit between the experimental data (symbols) and the theoretical data (solid lines) for the complex proton transfer reaction.

In our earlier study[1i] we were able to assign microscopic rate constants for four different radical cation proton transfer reactions carried out at 291 K. The values of KIE_{real} in these four reactions ranged from 31 to 47, all significantly larger than the semi-classical maximum value of about 10 under the reaction conditions.[19] In the present study we confine our attention to the reactions of a single radical cation, $DMA^{+\bullet}$, with 2 different pyridine bases (LUT and DEP) over a range of temperatures.

The experimental criteria most often considered[20–22] to implicate tunneling in proton transfer reactions are still those listed by Bell (values in parentheses refer to the C–H bond at 298 K); (a) KIE which exceed the value predicted by semi-classical theory (≅10), (b) $E_a^D - E_a^H$ which exceed the isotopic difference in zero-point energies (≅1.35 kcal mol^{-1}) and (c) A^D/A^H which exceed the corresponding semi-classical values (0.7–1.2).[16] Clearly, as demonstrated by the data in Tables 3 and 4, KIE_{real} for both reactions comply with criterion (a). The values of KIE_{real} for the two reactions range from 62–189 and 76–247 and increase significantly with decreasing temperature. Likewise, criterion (b) is fulfilled by data for both reactions. When the base was DEP in dichloromethane–Bu_4NPF_6 (0.2 M) (Table 4), $E_a^D - E_a^H$ was observed to be equal to 4.07 kcal mol^{-1}, which is significantly larger than the semi-classical value. This quantity was found to be equal to 3.04 kcal mol^{-1} for the reaction of $DMA^{+\bullet}$ with LUT in acetonitrile–Bu_4NPF_6 (0.1 M) (Table 5), consistent with criterion (b). Activation data for the former reaction are clearly consistent with criterion (c), with A^D/A^H equal to 17.6. The ratio for the latter reaction ($A^D/A^H = 1.83$) is somewhat lower but still consistent with this criterion.

It is also of interest to apply the tunneling criteria to KIE_{app} and the activation parameters derived from $k_{app}{}^H$ and $k_{app}{}^D$. When the base was DEP in dichloromethane–Bu_4NPF_6 (0.2 M), KIE_{app} values were only slightly greater than the semi-classical maximum value. The activation energy difference ($E_a^D - E_a^H$) was equal to 1.16 kcal mol^{-1}, which is very close to that predicted by semi-classical theory and this is also the case for A^D/A^H (= 0.95). For the reaction of $DMA^{+\bullet}$ with LUT in acetonitrile–Bu_4NPF_6 (0.1 M) KIE_{app} values are sufficiently large to suggest tunneling, while the activation parameters are consistent with semi-classical behavior. Thus, a strong case for significant proton tunneling could not be made for either reaction from relationships developed from the apparent rate constants.

We appear to be justified in concluding that the reactions of $DMA^{+\bullet}$ with both bases are accompanied by extensive proton tunneling. Also, it is clear that without resolving the proton transfer kinetics this conclusion could not be arrived at. The KIE_{real} observed for these two reactions are among the largest that have been reported for proton transfer reactions.

A question may arise as to whether or not the large degree of tunneling observed for these reactions is connected to some special property of radical cation proton transfer reactions. On the basis of the limited data available we are unable to conclude whether or not radical cation reactions are especially subject to tunneling effects. It is our opinion that reactions involving the cleavage of C–H bonds, whether H leaves as a proton, a hydrogen atom or a hydride ion, may follow two-step mechanisms, of which eqns. (2)–(4) is an example, where formation of an association complex is kinetically significant. Depending upon the relative magnitudes of the microscopic rate constants, KIE_{real}/KIE_{app} can vary from unity to >100,[1i] which highlights the importance of insuring that KIE_{real} are used when assessing the degree of tunneling in a reaction. Thus, it appears to be likely that many of the KIE_{app} which have been reported for C–H proton transfer are not equivalent to KIE_{real}. This being the case, the degree of tunneling in these reactions remains unknown and comparisons with radical cation proton transfer reactions cannot be made. The proton transfer reaction between $NPPE_{H(D)}$ and hydroxide ion[16] mentioned earlier supports the latter conclusion. A large number of kinetic studies have been carried out on the proton transfer reactions of nitroalkanes,[22–46] of which $NNPE_{H(D)}$ is a representative example, with the common assumption that the mechanism involves the simple reversible proton transfer without any intermediates. Our studies on the proton transfer reactions of $NNPE_{H(D)}$ with hydroxide ion in aqueous acetonitrile[16] suggest that the latter assumption is not justified and that the deuterium kinetic isotope effects reported are KIE_{app} which may be very much lower than KIE_{real}.

Another relevant question deals with whether or not radical cation proton transfer reactions reach steady-state at a later stage than occurs with other C–H cleavage reactions. This is very important in terms of being able to assess whether or not KIE_{app} values are reasonable approximations to KIE_{real}. We believe that the answer to this question is a definitive no. The proton transfer reaction[16] of $NNPE_{H(D)}$ mentioned in the previous paragraph, as well as an apparent hydride transfer reaction[47] that we have observed to follow the complex mechanism, are pertinent examples. Both of the latter involve complex mechanisms for reactions that do not reach steady-state until late in the first half-life.

Some of the largest deuterium kinetic isotope effects which have been reported involve unimolecular hydrogen atom shift in free radicals.[48–53] In the case of unimolecular reactions the formation of a reactant complex is not a necessary feature of the mechanism and it is likely that KIE_{app} are very nearly the same as KIE_{real} for single-step reactions. The fact that tunneling can be implicated from the very large KIE that are often observed in these reactions, while tunneling can less frequently be shown for second-order reactions, suggests that KIE_{app} for the latter cannot usually be equated to KIE_{real} and are not reliable measures of the degree of tunneling.

Kreevoy and Kotchevar[54] have proposed a two-step mechanism for hydride transfer reactions. The first step involves complex–solvent relaxation before the hydride transfer event. They observed that KIE_{app} vary by about a factor of two as the solvent is changed over a range of aprotic and hydroxylic solvents and attribute the two extremes to slow and fast relaxing solvents. Their results suggest that extent of reaction dependent KIE_{app} may be observed for reactions experiencing this phenomenon providing that the kinetics can be studied in the time regime before steady-state is reached. We have observed[24] extent of reaction dependent KIE_{app} in a formal hydride transfer reaction and are currently studying the kinetics of this system.[47]

There is still far too little resolved kinetic data available to draw any firm conclusions concerning structural or solvent effects on the various rate constants [eqns. (2)–(4)] for the proton transfer reactions between radical cations and bases. The limited data do suggest some points of interest with regard to the association reactions between radical cations and bases. Data are available for the reactions of $DMA^{+\bullet}$ with LUT in acetonitrile (this study) and in dichloromethane.[1i] The association constants ($K_{eq} = k_f/k_b$) are equal to 16.5 (292 K) and 25.0 (291 K), respectively, in the two solvents, indicating a small solvent effect. In dichloromethane, K_{eq} was observed to be equal to 25.0 (291 K) when the base is LUT and 10.0 (292 K) when the base is DEP. The latter suggests a steric effect for the formation of the radical cation–base complexes. This is also reflected in the relative values of binding energies of the corresponding radical cation–base complexes; −1.2 and −0.6 kcal mol^{-1} for LUT in acetonitrile–Bu_4NPF_6 (0.1 M) and DEP in dichloromethane–Bu_4NPF_6 (0.2 M), respectively.

The rate constants for the formation of the intermediate complexes (k_f) are moderate; 7.94×10^4 M^{-1} s^{-1} for the reaction of LUT and 3.42×10^3 M^{-1} s^{-1} for the reaction of DEP with $DMA^{+\bullet}$. Clearly, the complexes are not encounter complexes that form upon diffusion of the reactants together. It appears reasonable to assume that the encounter complexes rearrange to reactant complexes in which the reactants and the solvent molecules are oriented to favor the proton transfer step. This added detail cannot be verified by kinetic studies.

Conclusions

Extent of reaction dependent KIE_{app} for the reactions of $DMA^{+\bullet}$/$DMA\text{-}d_6^{+\bullet}$ with both DEP and LUT were observed over the entire range of temperature studied. Excellent fit between experimental R_I'/log (1/v) response curves and those from theoretical data obtained by digital simulation were observed in all cases. This allowed microscopic rate constants to be assigned for all reactions. The resulting KIE_{real} were observed to be much larger than predicted by semi-classical theory. The activation parameter quantities ($E_a^D - E_a^H$ and A^D/A^H) were also consistent with significant proton tunneling contributions to the reactions. Our studies on proton transfer reactions of radical cations have thus far dealt with alkylanthracene radical cations reacting with pyridine bases. Extension of the two-step mechanism to include other radical cation–base systems will require further investigation. Further systematic studies of steric and solvent effects on the extent of tunneling in radical cation proton transfer reactions are expected to provide more detail on this phenomenon.

Experimental

Materials

Dichloromethane was allowed to reflux for several hours over $CaCl_2$ and, after passing through active neutral alumina, was used without further purification. Acetonitrile was distilled from P_2O_5 and used without further purification after passing through neutral alumina to remove traces of water. DMA (Aldrich) was recrystallized from propan-2-ol. $DMA\text{-}d_6$ was prepared according to a literature procedure[55] using methyl-d_3-magnesium iodide (99.5+%) as the Grignard reagent. 2,6-Dimethylpyridine (99.5+%, Aldrich) was distilled under reduced pressure before use. 2,6-Diethylpyridine was prepared according to a literature method[56] and further purified by column chromotography (silica gel) before use.

Instrumentation and procedures

The instruments and data handling procedures as well as the procedures used for kinetic measurements were those recently described.[1i] The digital simulations and the fitting of experimental to theoretical data were the same as recently reported.[1i] The R'_I range for the kinetic measurements was restricted to that where the experimental data are most reliable (0.85–0.50). Above 0.85 the R'_I/(1/v) response curve is relatively flat giving rise to larger experimental errors. At R'_I lower than about 0.5, the reverse peak on a cyclic voltammogram is no longer observed and changes in R'_I with v reflect only the increase in height of the peak for the forward charge transfer process.

Acknowledgements

Acknowledgement is made to the donors of The Petroleum Research Fund, administered by the ACS, as well as to the National Science Foundation (CHE-970835 and CHE-0074405) for support of this research.

References

1 (*a*) J. Barek, E. Ahlberg and V. D. Parker, *Acta Chem. Scand., Ser. B*, 1980, **34**, 85; (*b*) R. Schmid Baumberger and V. D. Parker, *Acta Chem. Scand., Ser. B*, 1980, **34**, 537; (*c*) V. D. Parker, *Acta Chem. Scand., Ser. B*, 1985, **39**, 227; (*d*) V. D. Parker and M. Tilset, *J. Am. Chem. Soc.*, 1986, **108**, 6371; (*e*) B. Reitstöen and V. D. Parker, *J. Am. Chem. Soc.*, 1990, **112**, 4968; (*f*) V. D. Parker, Y. Chao and B. Reitstöen, *J. Am. Chem. Soc.*, 1991, **113**, 2336; (*g*) J.-Y. Xue and V. D. Parker, *J. Org. Chem.*, 1994, **59**, 6564; (*h*) V. D. Parker, Y.-T. Chao and G. Zheng, *J. Am. Chem. Soc.*, 1997, **119**, 11390; (*i*) V. D. Parker, Y. Zhao, Y. Lu and G. Zheng, *J. Am. Chem. Soc.*, 1998, **120**, 12720.

2 (*a*) C. J. Schlesener, C. Amatore and J. K. Kochi, *J. Am. Chem. Soc.*, 1984, **106**, 3567; (*b*) C. J. Schlesener, C. Amatore and J. K. Kochi, *J. Am. Chem. Soc.*, 1984, **106**, 7472; (*c*) C. J. Schlesener, C. Amatore and J. K. Kochi, *J. Phys. Chem.*, 1986, **90**, 3747; (*d*) S. Sankararaman, S. Perrier and J. K. Kochi, *J. Am. Chem. Soc.*, 1989, **111**, 6448; (*e*) J. M. Masnovi, S. Sankararaman and J. K. Kochi, *J. Am. Chem. Soc.*, 1989, **111**, 2263; (*f*) T. M. Bockman, Z. J. Karpinski, S. Sankararaman and J. K. Kochi, *J. Am. Chem. Soc.*, 1992, **114**, 1970; (*g*) T. M. Bockman, S. M. Hubig and J. K. Kochi, *J. Am. Chem. Soc.*, 1998, **120**, 2826.

3 (*a*) S. Fukuzumi, Y. Kondo and T. Tanaka, *J. Chem. Soc., Perkin Trans. 2*, 1984, 673; (*b*) S. Fukuzumi, Y. Tokuda, T. Kitano, T. Okamoto and J. Otera, *J. Am. Chem. Soc.*, 1993, **115**, 8960.

4 (*a*) L. M. Tolbert and R. K. Khanna, *J. Am. Chem. Soc.*, 1987, **109**, 3477; (*b*) L. M. Tolbert, R. K. Khanna, A. E. Popp, L. Gelbaum and L. A. Bottomley, *J. Am. Chem. Soc.*, 1990, **112**, 2373; (*c*) L. M. Tolbert, R. K. Khanna, A. E. Popp, L. Gelbaum and L. A. Bottomley, *J. Am. Chem. Soc.*, 1990, **112**, 2373.

5 (*a*) J. P. Dinnocenzo and T. E. Banach, *J. Am. Chem. Soc.*, 1989, **111**, 8646; J. P. Dinnocenzo and T. E. Banach, *J. Am. Chem. Soc.*, 1989,

111, 2263; (*b*) J. P. Dinnocenzo, S. B. Karki and J. P. Jones, *J. Am. Chem. Soc.*, 1993, **115**, 7111.
6 (*a*) E. Baciocchi, M. Mattioli, R. Romano and R. Ruzziconi, *J. Org. Chem.*, 1991, **56**, 7154; (*b*) E. Baciocchi, T. D. Giacco and F. Elisei, *J. Am. Chem. Soc.*, 1993, **115**, 12290; (*c*) E. Baciocchi, M. Bietti, L. Putignani and S. Steenken, *J. Am. Chem. Soc.*, 1996, **118**, 5952; (*d*) E. Baciocchi, M. Bietti and S. Steenken, *J. Am. Chem. Soc.*, 1997, **119**, 4078; (*e*) M. Bietti, E. Baciocchi and S. Steenken, *J. Am. Chem. Soc.*, 1998, **120**, 7337; (*f*) E. Baciocchi, T. Del Giacco, F. Elisei and O. Lanzalunga, *J. Am. Chem. Soc.*, 1998, **120**, 11800.
7 (*a*) W. Xu and P. S. Mariano, *J. Am. Chem. Soc.*, 1991, **113**, 1431; (*b*) W. Xu, X.-M. Zhang and P. S. Mariano, *J. Am. Chem. Soc.*, 1991, **113**, 8863.
8 J. Steadman and J. A. Syage, *J. Am. Chem. Soc.*, 1991, **113**, 6786.
9 (*a*) P. Hapiot, J. Moiroux and J.-M. Saveant, *J. Am. Chem. Soc.*, 1990, **112**, 1337; (*b*) A. Anne, P. Hapiot, J. Moiroux, P. Neta and J.-M. Saveant, *J. Phys. Chem.*, 1991, **95**, 2370; (*c*) A. Anne, P. Hapiot, J. Moiroux, P. Neta and J.-M. Saveant, *J. Am. Chem. Soc.*, 1992, **114**, 4694; (*d*) A. Anne, S. Fraoua, P. Hapiot, J. Moiroux and J.-M. Saveant, *J. Am. Chem. Soc.*, 1995, **117**, 7412; (*e*) A. Anne, S. Fraoua, V. Grass, J. Mouroux and J.-M. Saveant, *J. Am. Chem. Soc.*, 1998, **120**, 2951.
10 (*a*) A. M. Nicholas and D. R. Arnold, *Can. J. Chem.*, 1982, **60**, 2165; (*b*) A. M. Nicholas, R. J. Boyd and D. R. Arnold, *Can. J. Chem.*, 1982, **60**, 3011.
11 (*a*) F. G. Bordwell and J.-P. Cheng, *J. Am. Chem. Soc.*, 1989, **111**, 1792; (*b*) X. Zhang and F. G. Bordwell, *J. Org. Chem.*, 1992, **57**, 4163; (*c*) X. Zhang, F. G. Bordwell, J. E. Bares, J.-P. Cheng and B. C. Petrie, *J. Org. Chem.*, 1993, **58**, 3051.
12 V. D. Parker, *Acc. Chem. Res.*, 1984, **17**, 243.
13 (*a*) A. Pross, *J. Am. Chem. Soc.*, 1986, **108**, 3537; (*b*) S. S. Shaik and A. Pross, *J. Am. Chem. Soc.*, 1989, **111**, 4306.
14 (*a*) V. D. Parker and M. Tilset, *J. Am. Chem. Soc.*, 1987, **109**, 2521; (*b*) B. Reitstöen, F. Norrsell and V. D. Parker, *J. Am. Chem. Soc.*, 1989, **111**, 8463; (*c*) V. D. Parker, B. Reitstöen and M. Tilset, *J. Phys. Org. Chem.*, 1989, **2**, 580; (*d*) B. Reitstöen and V. D. Parker, *J. Am. Chem. Soc.*, 1991, **113**, 6954; (*e*) V. D. Parker, K. L. Handoo and B. Reitstöen, *J. Am. Chem. Soc.*, 1991, **113**, 6218; (*f*) V. D. Parker and M. Tilset, *J. Am. Chem. Soc.*, 1991, **113**, 8778; (*g*) D. Bethell and V. D. Parker, *J. Phys. Org. Chem.*, 1992, **5**, 317; (*h*) B. Reitstöen and V. D. Parker, *Acta Chem. Scand.*, 1992, **46**, 464; (*i*) V. D. Parker, M. Pedersen and B. Reitstöen, *Acta Chem. Scand.*, 1993, **47**, 560; (*j*) V. D. Parker, K. L. Handoo and F. Norrsell, *J. Org. Chem.*, 1993, **58**, 4929.
15 (*a*) M. S. Workentin, N. P. Schepp, L. J. Johnston and D. D. M. Wayner, *J. Am. Chem. Soc.*, 1994, **116**, 1141; (*b*) M. S. Workentin, L. J. Johnston, D. D. M. Wayner and V. D. Parker, *J. Am. Chem. Soc.*, 1994, **116**, 8279; (*c*) M. S. Workentin, T. L. Morkin, V. D. Parker and D. D. M. Wayner, *J. Phys. Chem. A*, 1998, **102**, 6503.
16 Y. Zhao, Y. Lu and V. D. Parker, *J. Am. Chem. Soc.*, 2001, **123**, 1579.
17 R. P. Bell *The Tunnel Effect in chemistry*, Chapman & Hall, London, 1980.
18 (*a*) V. D. Parker, *Electroanal. Chem.*, 1983, **19**, 131; (*b*) E. Ahlberg and V. D. Parker, *J. Electroanal. Chem.*, 1981, **121**, 57.
19 M. Rudolph, D. P. Reddy and S. W. Feldberg, *Anal. Chem.*, 1994, **66**, 589A and references cited therein.
20 R. P. Bell, *Chem. Soc. Rev.*, 1974, **3**, 513.
21 S. Wolf, S. Hoz, C.-K. Kim and K. Yang, *J. Am. Chem. Soc.*, 1990, **112**, 4186.
22 E. F. Caldin and J. C. Trickett, *Trans. Faraday Soc.*, 1953, **49**, 772.
23 E. S. Lewis and L. H. Funderburk, *J. Am. Chem. Soc.*, 1967, **89**, 2322.
24 F. G. Bordwell, W. J. Boyle and K. C. Yee, *J. Am. Chem. Soc.*, 1970, **92**, 5926.
25 E. F. Caldin, A. Jarczewski and K. T. Leffek, *Trans. Faraday Soc.*, 1971, **67**, 110.
26 A. Jarczewski and K. T. Leffek, *Can. J. Chem.*, 1972, **50**, 24.
27 J.-H. Kim and K. T. Leffeck, *Can. J. Chem.*, 1974, **52**, 592.
28 E. F. Caldin and S. Mateo, *J. Chem. Soc., Chem. Commun.*, 1973, 854.
29 E. F. Caldin and S. Mateo, *J. Chem. Soc., Faraday Trans. 1*, 1975, **71**, 1876.
30 A. Jarczewski and P. Pruszynski, *Can. J. Chem.*, 1975, **53**, 1176.
31 E. F. Caldin, E. Dawson and R. M. Hyde, *J. Chem. Soc., Faraday Trans. 1*, 1975, **71**, 528.
32 F. G. Bordwell and W. J. Boyle, *J. Am. Chem. Soc.*, 1970, **97**, 3447.
33 O. Rogne, *Acta Chem. Scand.*, 1978, 559.
34 A. Jarczewski, P. Pruszynski and K. T. Leffek, *Can. J. Chem.*, 1979, **57**, 669.
35 A. J. Kresge and M. F. Powell, *J. Am. Chem. Soc.*, 1981, **103**, 201.
36 E. F. Caldin, S. Mateo and P. Warrick, *J. Am. Chem. Soc.*, 1981, **103**, 202.
37 N. Sugimoto, M. Sasaki and J. Osugi, *J. Phys. Chem.*, 1982, **86**, 3418.
38 A. Jarczewski, P. Pruszynski and K. T. Leffek, *Can. J. Chem.*, 1983, **61**, 2029.
39 N. Sugimoto, M. Sasaki and J. Osugi, *Bull. Chem. Soc. Jpn.*, 1984, **57**, 366.
40 P. Pruszynski and A. Jarczewski, *J. Chem. Soc., Perkin Trans. 2*, 1986, 1117.
41 K. T. Leffek and P. Pruszynski, *Can. J. Chem.*, 1988, **66**, 1454.
42 W. Galezowski and A. Jarczewski, *J. Chem. Soc., Perkin Trans. 2*, 1989, 1647.
43 K. T. Leffek, P. Pruszynski and K. Thanapaalasingham, *Can. J. Chem.*, 1989, **67**, 590.
44 A. J. Kresge and M. F. Powell, *J. Phys. Org. Chem.*, 1990, **3**, 55.
45 W. Galezowski and A. Jarczewski, *Can. J. Chem.*, 1990, **68**, 2242.
46 A. Jarczewski, G. Schroeder and K. T. Leffek, *Can. J. Chem.*, 1991, **69**, 468.
47 Y. Lu, Y. Zhao, Z. Shen and V. D. Parker, unpublished work.
48 S. N. Smirnov, N. S. Golubev, G. S. Denisov, H. Benedict, P. Schah-Mohammedi and H.-H. Limbach, *J. Am. Chem. Soc.*, 1996, **118**, 4094.
49 W. Siebrand, T. A. Wildman and M. Z. Zgierski, *J. Am. Chem. Soc.*, 1984, **106**, 4089.
50 G. Brunton, J. A. Gray, D. Griller, L. R. C. Barclay and K. U. Ingold, *J. Am. Chem. Soc.*, 1978, **100**, 4197.
51 K.-H. Grellman, H. Weller and E. Tauer, *Chem. Phys. Lett.*, 1983, **95**, 195.
52 K.-H. Grellman, U. Schmitt and H. Weller, *Chem. Phys. Lett*, 1982, **88**, 40.
53 H.-H. Limbach, J. Henning, D. Gerritzen and H. Rumpel, *Faraday Discuss. Chem. Soc.*, 1982, **74**, 229.
54 (*a*) M. M. Kreevoy and A. T. Kotchevar, *J. Am. Chem. Soc.*, 1990, **112**, 3579; (*b*) A. T. Kotchevar and M. M. Kreevoy, *J. Phys. Chem.*, 1991, **95**, 10345.
55 L. F. Fieser and H. Heymann, *J. Am. Chem. Soc.*, 1942, **64**, 372.
56 L. J. Durham and D. J. McLeod, *Org. Syn.*, 1963, **Coll. Vol. IV**, 510.